EARTH SURFACE PROCESSES AND LANDFORMS, VOL. 14, 597–614 (1989)

A POSSIBLE CAUSAL RELATIONSHIP BETWEEN CREEP AND SLIDING ON RWAZA HILL, SOUTHERN RWANDA

J. MOEYERSONS
Royal Museum of Central Africa, B–1980 Tervuren, Belgium

Received 28 June 1988
Revised 17 January 1989

ABSTRACT

Stability calculations on a strongly creeping 28° slope on Rwaza Hill in Southern Rwanda reveal an apparent contradiction: terracette formation within the kaolinitic soil mantle should only be possible during hydrological conditions of high phreatic surfaces, for which the entire soil mantle should already have slid down in a translational sliding movement.

This apparent contradiction can only be explained if it is accepted that the soil shear resistance can fall temporarily below the residual soil shear strength. A creep experiment confirms the theoretical possibility of this hypothesis. Furthermore, the configuration of the sliding surfaces in the field, consisting in fact of lenses of crumbled earth, shows close affinities with the pattern of potential ruptures in a creeping soil as provided by rheological theory.

These data strongly suggest that, on natural slopes, creep should be the ultimate soil mechanical resason for sudden failures.

KEY WORDS Terracette Creep Slope stability Slip lines Sliding

INTRODUCTION

Rwanda is a hilly country, located in the centre of the African continent. It occupies the eastern shoulder of the western rift, at about 2° south of the equator. To the west, the country is bordered by Lake Kivu. Due to its elevation (1 000–3 000 m), Rwanda enjoys a rather mild climate, characterized by a mean annual temperature around 20°C and by two rainy seasons, from the middle of September to December and from the end of January till May or June respectively. At Butare (Figure 1), the mean annual precipitation amounts to more than 1 100 mm/year, but an important drop of rainfall amount, correlative to the last drought in Sahelian Africa, has been recorded at our experimental station at Rwaza Hill.

Like most hills in the area, Rwaza Hill is underlain by Precambrian phyllitic rocks, over which a non swelling kaolinitic soil has developed. This soil is characterized by the presence, if not eroded away, of a 50 cm or less thick humic A-horizon, sometimes buried below colluvial deposits. In general, a more clayey red subsoil exists below this horizon. Its thickness often exceeds 1·5 m. The difference in clay content between the humic horizon (12 per cent–19 per cent of particles smaller than 2 microns) and the red subsoil (23 per cent–33 per cent) partly explains the presence of a drop in the hydraulic conductivity at the transition between both horizons. Finally, a second drop in hydraulic conductivity exists near the base of the soil, where a 10 to 50 cm thick gravelly–clayey layer forms the transition between the red subsoil and the phyllitic bedrock, often weathered *in situ*. Percolation at both levels of decreasing hydraulic conductivity is evidenced by the presence of macropores, cavities, and suffosion tunnels, active during and after heavy rains, especially in the second half of the big rain season in May and June (Figure 2).

0197–9337/89/070597–18$09.00

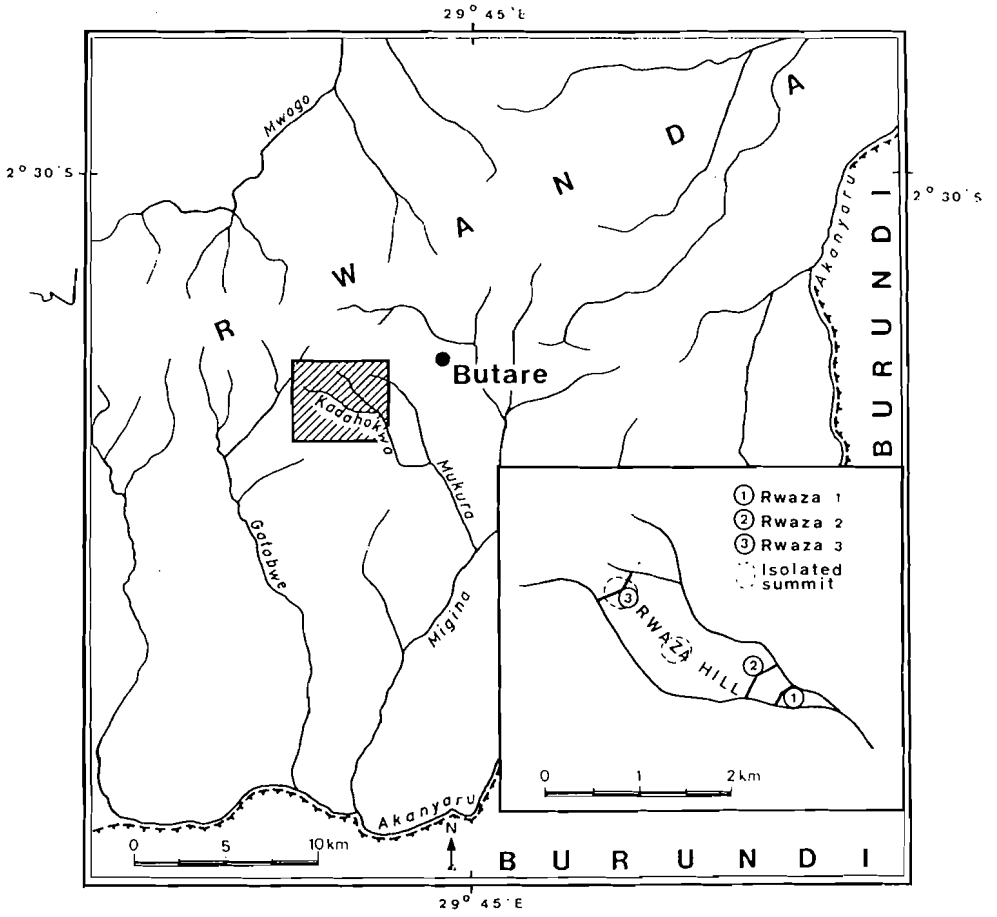

Figure 1. Localization map of Rwaza Hill in Southern Rwanda

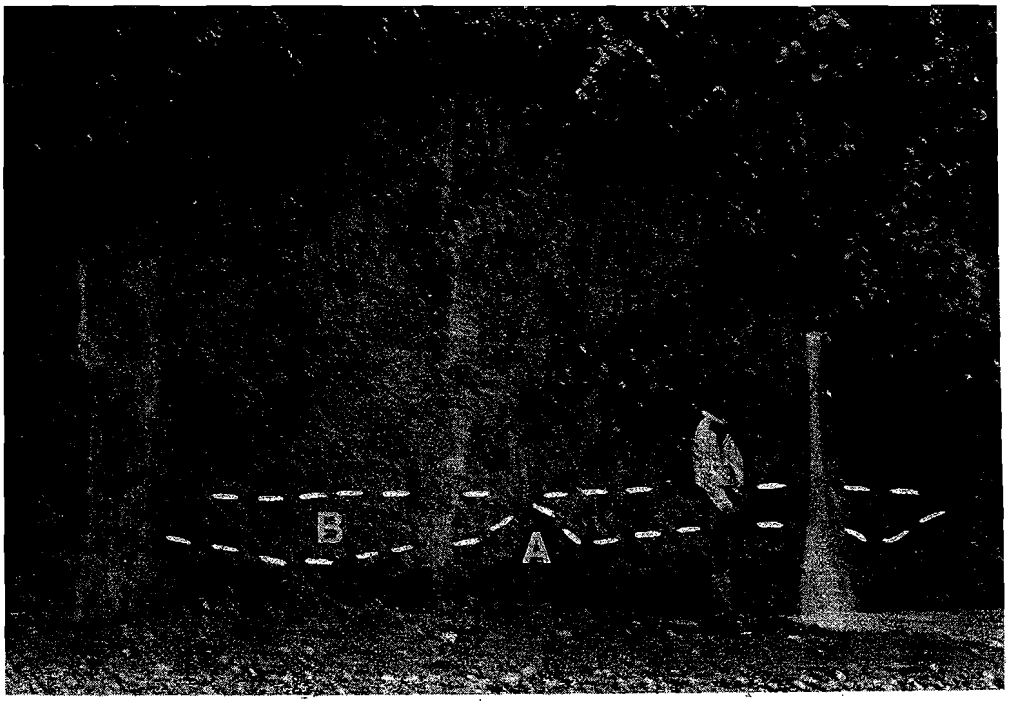

Figure 2. Three types of runoff visible during a heavy rain in a road cut at Nyange (Kivumu): 1. Surface runoff cascading over the wall; 2. Tunnel stormrunoff; 3. Diffuse percolation in A and B, A being the basal clayey–gravelly layer

Soil use at Rwaza Hill is essentially dictated by subsistent agricultural activities, resulting in an irregular mosaic of parcels of cultivated land, bananas, harricots, cassawa, sweet potatoes . . . , interrupted by often overgrazed pasture ground, fallow land, and over-exploited eucalyptus tree plantations.

MASS MOVEMENTS

From observations throughout the country and from detailed long-term measurements on Rwaza Hill (Figure 1), it appears that creep is a very important geomorphological process, affecting most hill sides, especially when developed on phyllitic rocks. This is illustrated on Figure 3, where 7 year changes in distances between 60 cm long iron stakes, inserted into the soil along three cross-profiles on Rwaza Hill, are indicated.

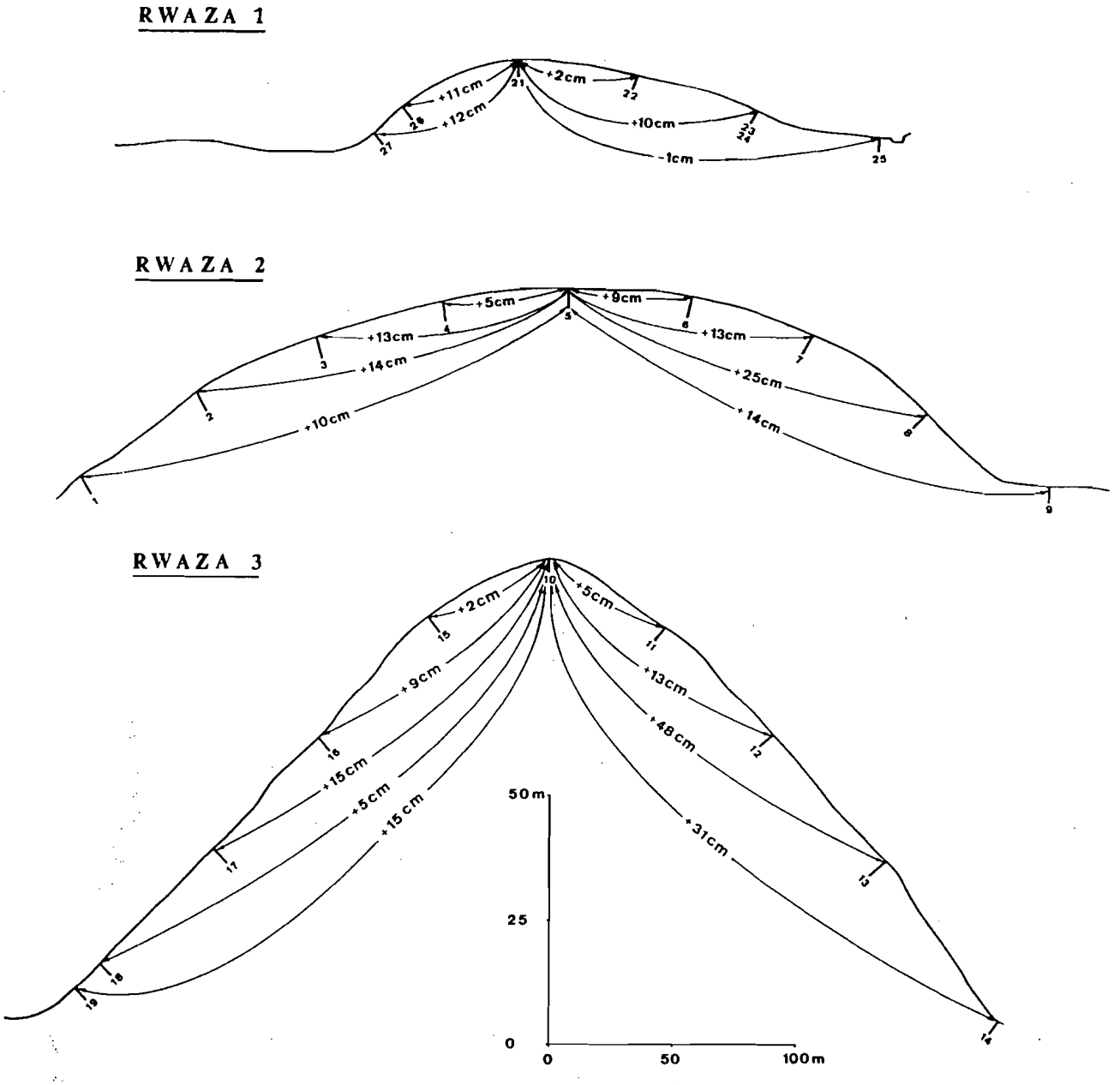

Figure 3. Distances between iron stakes, inserted into the soil in 1977 had undergone important changes in 1984. Rwaza Hill, measurements along three cross-sections

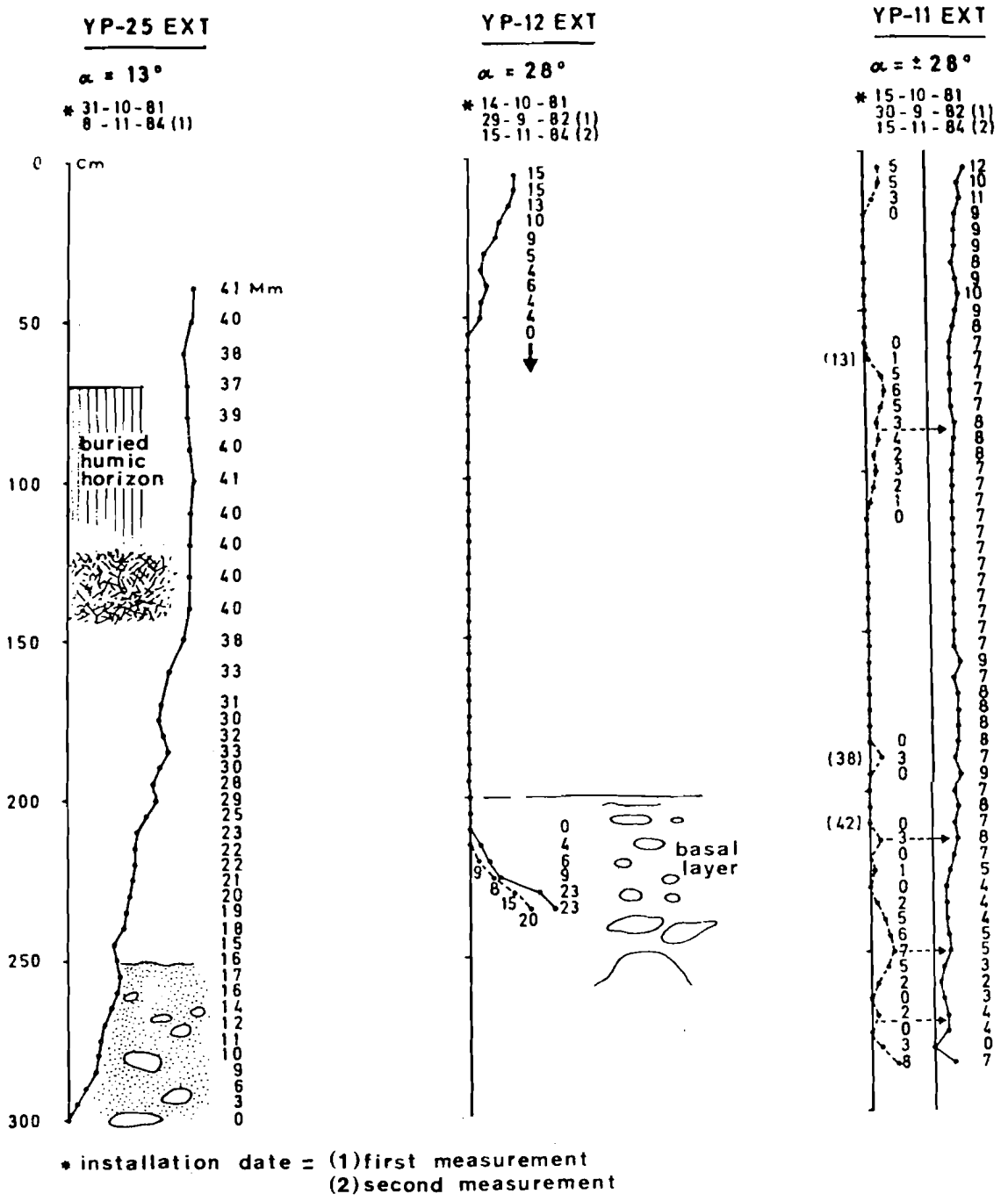

Figure 4. Rwaza Hill: the relative displacement component parallel to the surface, of tracers in the wall of three deep Young pits

Tracer displacements in deep Young pits (Young, 1960) show that creep generally affects the soil over its entire thickness, an important proportion of the total movement being located within the gravelly–clayey basal horizon, even when situated at a depth of 3 m (Figure 4). A second creep maximum is often situated near the top of the soil profile, whether the humic soil horizon is present or not.

It frequently happens, at the end of the big rain season (May, June), that important portions of steep (more than 25°) creeping slopes suddenly fail. Figure 5 gives an example of a bottle slide, 5 km to the west of Butare. One head of the slide has been completely emptied, while the other head is shoked by the only slightly displaced soil mass. As a general rule, the major plane of rupture coincides with the basal gravelly–clayey layer

Figure 5. Bottle slide, about 10 km to the west of Butare. Note the presence of terracettes, visible everywhere, except on the cultivated parcel

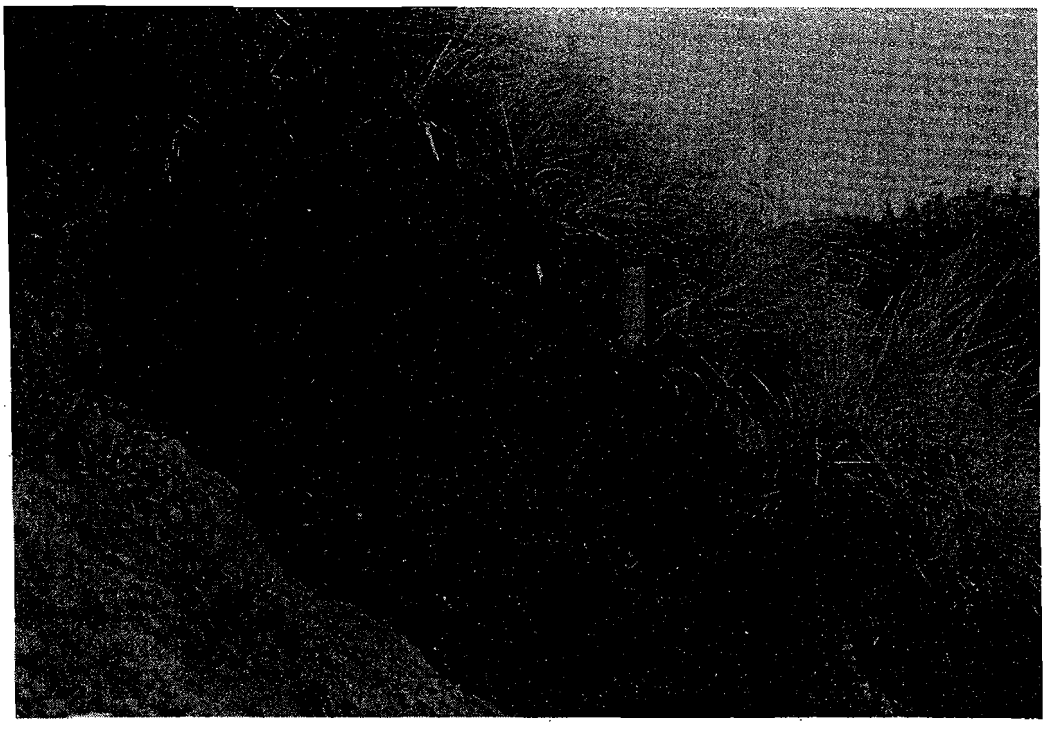

Figure 6. Trench crossing terracettes, showing how they are separated not by single fissures but by lenses of crumbled earth, underlined on the pit wall. The p.v.c. tube is 30 cm long

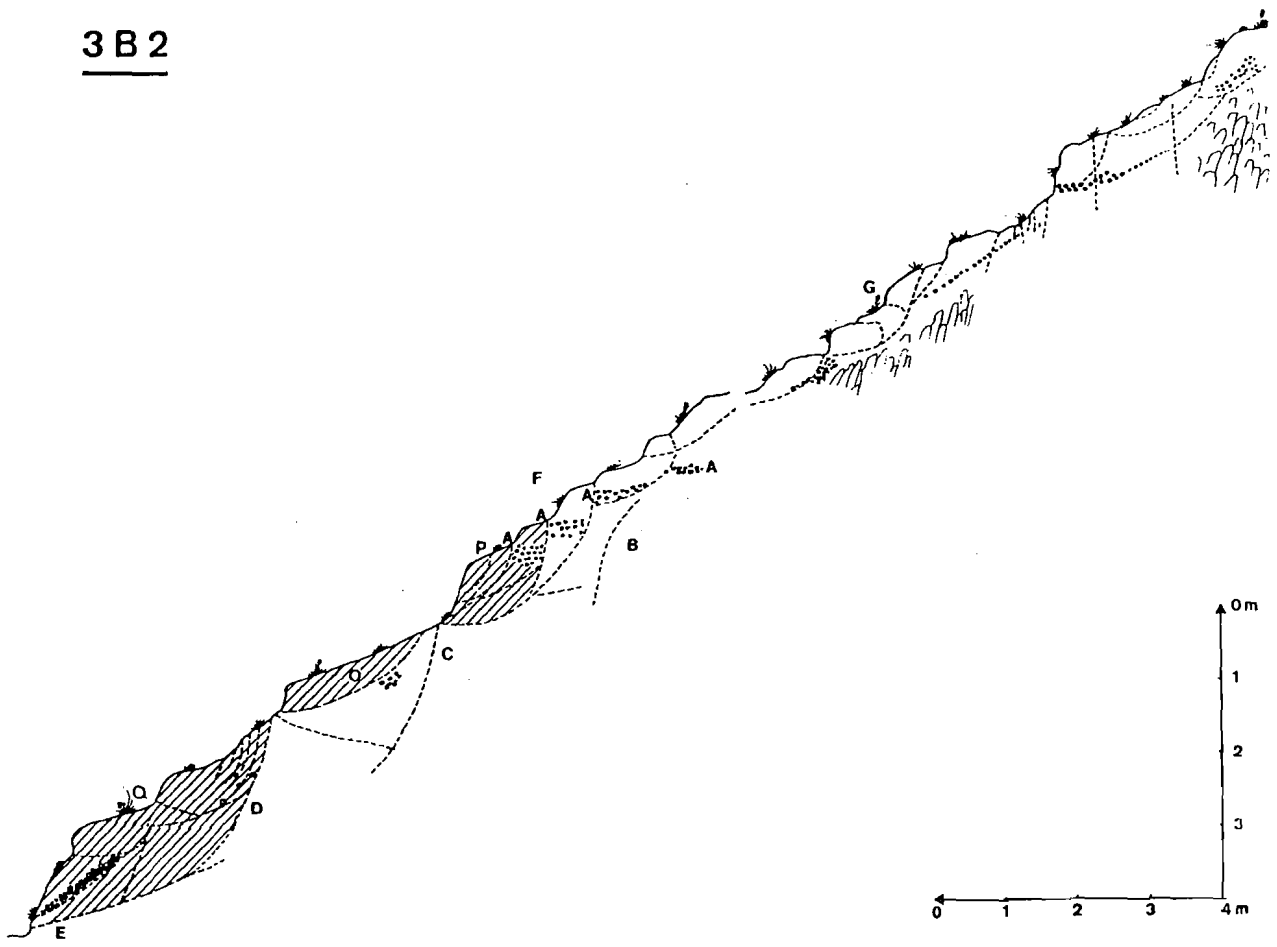

Figure 7. Trench 3B2 on Rwaza 3B. The configuration of supposed slide planes in relation to the terracette topography

on top of the bedrock. It is also very common that creeping slopes, affected by sudden failures, display a terracette topography around the slide scars. From trenches into these terracettes it appears that they are built up by individual soil pillars bended forward near the soil surface and separated by curved fissures, which are, in fact, curved lenses of crumbled earth (Figure 6).

More detailed information about the relation between soil structures and terracettes could be gained on the 28° steep side of Rwaza 3B (Figure 3), where also small slidings have occurred and where the whole slope shows a typical terracette morphology. It appears (Figure 7) in trench 3B2 that the microtopography of the slope into its slightest detail can be correlated with the presence of fissures and lenses of crumbled earth, showing a pattern typical for slumped structures. The fact that some local stone lines (A) are dislocated along curved fissured lenses is the ultimate stratigraphical proof that the terracettes are to be considered as serial slumpings.

Measurements along tracer lines, composed of aluminium blades (5 cm × 5 cm × 0·05 cm) crossing a number of supposed slide surfaces at right (two cases) and obtuse (three cases) angles indicate slow sliding of the order of some millimetres a year.

SOIL MECHANICAL PARAMETERS FROM THE SOIL AT RWAZA HILL AND SLOPE STABILITY ANALYSES: AN APPARENT CONTRADICTION

On Rwaza Hill a Torvane shear device and a soil sheargraph (cohron sheargraph) were used to determine, in a number of locations, the *in situ* values of apparent cohesion and angle of apparent internal friction.

Two points have to be made clear:

1. The soil sheargraph has been used in order to determine the apparent angle of internal friction (φ') as well as the apparent residual angle of internal friction (φ'_r). The procedure adopted was as follows. After insertion of the head into the soil wall, the apparatus was turned under a constant normal pressure till its head started to follow the rotation movement ($\pm$revolution). In this way, the apparent soil resistance corresponding to the exerted normal stress was indicated on the graph paper. After about 1 revolution, the tangential stress was released but the normal stress maintained. Along the generated rupture plane the residual resistance has been measured by turning the apparatus again until rotation of the head started again. During the whole operation the normal pressure was maintained at $\pm$ constant level. Repetition of this procedure in the close vicinity of the first measurement hole but at different normal stresses enabled to establish Mohr envelopes indicating $C'-$, $\varphi'-$, and C'_r-, φ'_r- values in not fissured ground. In the lenses of crumbled earth, $C'-$ and $\varphi'-$ values did not differ from C'_r- and φ'_r- values and were generally very close to the C'_r- and φ'_r- values measured in not fissured soil.
2. There are two reasons why the field tests by means of the soil sheargraph should be considered as drained tests.

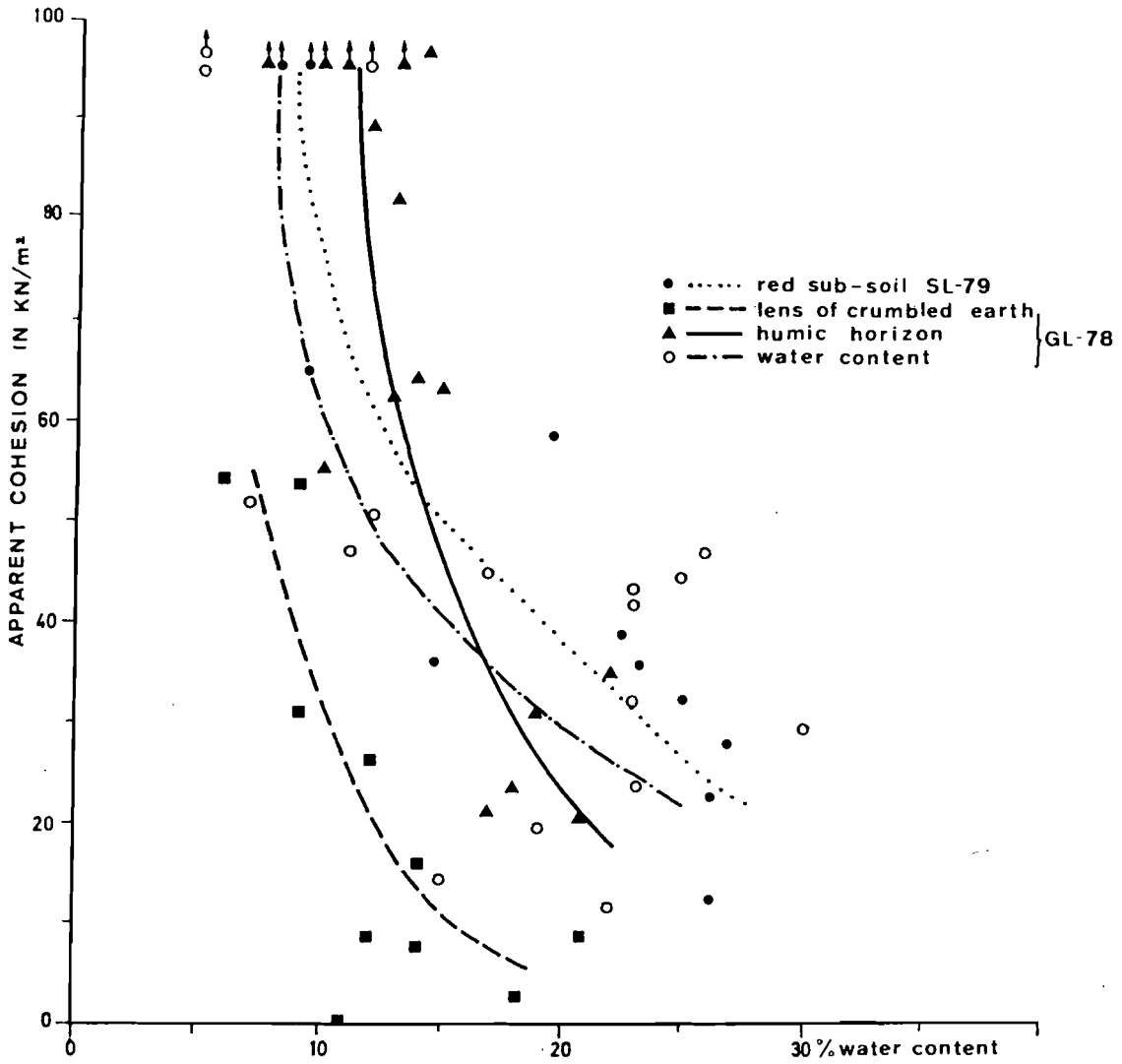

Figure 8. Torvane records of apparent cohesion in a number of artificial exposures at Rwaza Hill. Values from lenses of crumbed earth are close tp C'_r- values obtained by sheargraph tests

(a) The head of the soil sheargraph is only 5 mm high. This allows, even in clays of low permeability, a rapid dissipation of pore water pressures.
(b) In the laboratory, the results of consolidated drained tests obtained in the shearbox of a mono-axial shearing apparatus were compared with sheargraph tests on the same sample after its disruption in the shearbox. Most of the results are identical (Figure 11).

Figure 8 shows a decline of apparent cohesion with increasing water content of the soil in the different horizons. The apparent cohesion, determined in lenses of crumbled earth and composite fissures, lies markedly below the bundle of measurement points from the other undisturbed soil horizons. They form the so-called residual apparent cohesion.

Figure 9 illustrates a number of measurements of the angle of apparent internal friction in the red subsoil. Again, there is a general decrease with increasing water content, pointing to the possible role of suction in soil stability (Anderson *et al.*, 1987). And again, the angle of apparent residual internal friction, as determined in the lenses, appears below the bundle of not residual $\varphi'-$ values.

The stability of slopes in Rwanda can be considered from different points of view.

The infinite slope analysis

According to Skempton and Delory (1957), the safety factor F of an infinite slope can be expressed as the resisting forces, mobilized at the potential plane of failure, divided by the tractive forces along this plane:

$$F=\frac{\frac{C'_r}{\cos\alpha}+(\gamma_t \,.\, Z \,.\, \cos\alpha - Zm\cos\alpha\gamma_w)\tan\varphi'_r}{Z \,.\, \gamma_t \,.\, \sin\alpha} \tag{1}$$

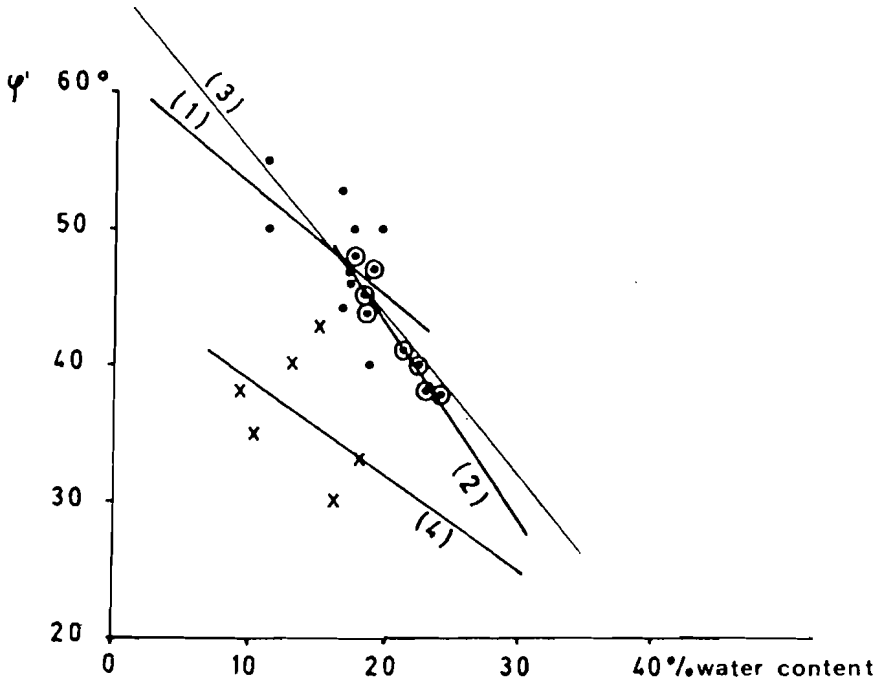

Figure 9. The apparent angle of internal friction, from records by means of the sheargraph. (1) and (2): φ' in not disturbed red subsoil, at a water content (w) respectively lower and higher than 18 per cent. (3): regression line for the (1) and (2) measurements together. (4): $\varphi'=\varphi'_r$ readings in lenses of crumbled earth.

Regression lines:

(2) $\varphi'=-1{\cdot}45\,w+72{\cdot}29 \quad r=-0{\cdot}95$
(3) $\varphi'=-1{\cdot}18\,w+67{\cdot}23 \quad r=-0{\cdot}80$
(4) $\varphi'_r=-0{\cdot}66\,w+44{\cdot}87 \quad r=-0{\cdot}43$

where C'_r = apparent residual cohesion
α = slope of the surface and failure plane, parallel to it
Z = the vertical depth of the potential failure plane
m = Z divided by the height of the phreatic surface above the potential failure plane
γ_t = bulk density of soil + water
γ_w = density of water
φ'_r = apparent residual angle of internal friction

If the values of Figures 8 and 9 are introduced in Equation 1, assuming that $F = 1$ (a slope on the verge of failure), two sliding characteristics can be determined:

1. The depth Z of the potential sliding plane. This has been done on Table I. Bulk densities are used as indicated. The $\varphi'-$ and $C'-$ values used are those close to saturation (water content = 33 per cent), but determined by a drained test. This represents a situation where a not saturated soil overlies the quasi saturated potential slip surface.
2. The threshold slope, on the verge of failure, if the residual apparent cohesion is considered to be zero. Table II summarizes a number of threshold slopes, determined by different $\varphi'-$ values and hydrological conditions imposed.

Table I. Calculated depths Z of the potential sliding planes for a number of slopes and a number of hydrological conditions

			$m=0$		$m=1$
Saturation degree	1·5%	15%	45%	88%	100%
Slope in degrees	z (ms) $\gamma_t = 14\ \mathrm{kN\,m^{-3}}$	z (ms) $\gamma_t = 14{\cdot}62\ \mathrm{kN\,m^{-3}}$	z (ms) $\gamma_t = 16\ \mathrm{kN\,m^{-3}}$	z (ms) $\gamma_t = 18\ \mathrm{kN\,m^{-3}}$	z (ms) $\gamma_t = 18{\cdot}54\ \mathrm{kN\,m^{-3}}$
14					3·67
15					2·18
16					1·56
17					1·21
18					1·00
19					0·85
20					0·74
21					0·66
22					0·59
23					0·54
24					0·50
25	7·05	6·75	6·17	5·59	0·46
26	3·56	3·41	3·11	2·77	
27	2·39	2·29	2·09	1·86	
28	1·81	1·73	1·59	1·41	
29	1·46	1·40	1·28	1·14	
30	1·23	1·18	1·08	0·96	0·36
31	1·07	1·02	0·93	0·83	
32	0·95	0·91	0·83	0·74	
33	0·85	0·81	0·74	0·66	
34	0·78	0·74	0·68	0·60	
35	0·71	0·68	0·62	0·56	
36					
37					
38					
39					0·29
40	0·53	0·51	0·46	0·41	0·25

Table I indicates that a slope of about 27° becomes already unstable from the moment that the failure surface, situated at a depth of about 2 m—the general depth of the gravelly–clayey basal layer, forming the failure belt in visited slides—is quasi saturated while the soil above still remains drier. Table II indicates that slopes steeper than 23°–24° can only remain stable when no water table develops in the soil. Wetting of the soil base close to saturation, even without establishment of pore water pressure, reduces the equilibrium slope to 23°–28°, depending on the introduction of φ' – values determined in undisturbed or fissured soil respectively.

The slight difference in threshold equilibrium slopes in both tables might be due to the fact that in the case of Table II the apparent residual cohesion, although very small, is neglected. However, both results are of the order of the threshold slope of about 25° observed in the field. In the light of the observation of active throughflow near the end of the big rain season (Figure 2), it is not surprising to observe in the field sudden failures as the calculations suggest. These results also indicate that the 28° slope of Rwaza 3B (Figure 7) occasionally is on the verge of failure. This is translated by accelerated creep (Figure 3).

Table II. Threshold slopes for different φ' – values for $m=0$ and $m=1$ condition. w = water content

Regression equations of Figure 9	φ'_r ($w=33\%$)	Threshold slope $m=0$ ($\tan\alpha=\tan\varphi'$)	Threshold slope $m=1$ ($\tan\alpha=\tan\varphi'/2$)
(3) $-1{\cdot}18\,w+67{\cdot}33$	28·59°	28·59° (54%)	15·24° (27%)
(2) $-1{\cdot}45\,w+72{\cdot}29$	24·24°	24·24° (45%)	12·80° (23%)
(4) $-0{\cdot}66\,w+44{\cdot}87$	23·09°	23·09° (43%)	12·03° (21%)

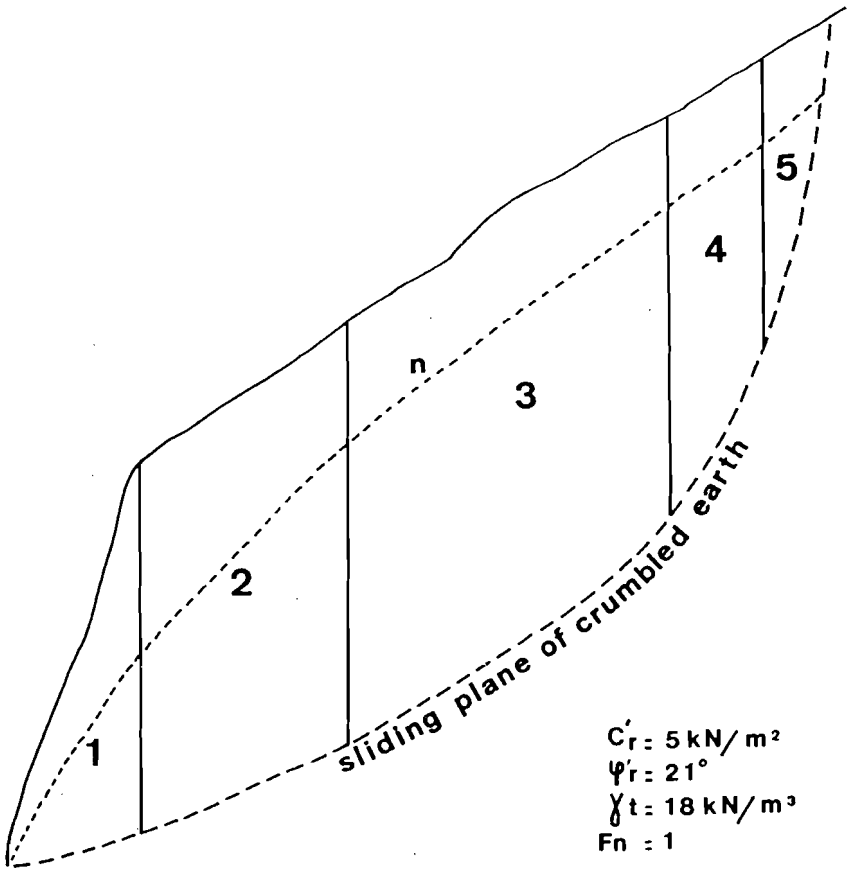

Figure 10. The terracette complex Q of Figure 7, restored in its supposed original position and divided into vertical slices. Stability calculations indicate a $F=1$ situation for the phreatic surface n, rising rather close to the surface

The stability of individual terracettes

Problems arise when stability calculations are applied to individual terracettes on Rwaza 3B. On Figure 7, terracette complexes for which stability conditions have been determined are shaded. As the slide surfaces are circular in form, the Swedish circle method (Fellnius, 1936) and the simplified Bishop method (Bishop, 1955) have been used.

On Figure 10, the case of terracette Q on Figure 7 is illustrated. The terracette is represented here in its supposed original position before sliding, thus before the development of the weak sliding surface. On Figure 8 it appears that C' for non fissured soil, at a water content of 30–33 per cent (saturation) corresponds to about 10 kN m^{-2}. In order to avoid overestimation of stability, a $C'-$ value of only 5 kN m^{-2} has been introduced. In the same way, the very low $\varphi'-$ value of 21° has been used. Nevertheless it appears, just as in some other cases tested, that the phreatic surface needs to rise close to the topographical surface before the stability factor F drops below unity.

This result is completely contradictory to the first set of stability calculations (Tables I and II) where, in the case of Rwaza 3B, translational sliding is suggested as soon as seepage occurs in the very lower part of the soil profile. In fact, the calculations on individual terracettes seem to indicate that terracette formation should only take place in hydrological conditions for which the soil mantle as a whole should already have slid down in a translational movement. This is, of course, impossible.

EFFECTS OF CREEP ON SOIL STRENGTH

It might be thought that rain can give rise to percolation in the base of the humic A-horizon, the deeper part of the soil profile remaining dry. This indeed, could partly explain the phenomenon. But a number of field observations show terracette formation around areas of sudden failures, on slopes where the humic A-horizon does not exist anymore. Therefore, it was felt that other explanations should be sought for the apparent contradiction concerning the stability of steep slopes in Rwanda.

Because of the importance of creep on the slopes considered, and in order to solve the problem, the effects of creep on soil mechanical parameters have been investigated. Emphasis is put on two points.

Creep as a possible factor of soil fatigue at Rwaza

Zaruba and Mencl (1976) mention that soil can fail when prolonged strain is induced by shear stresses below the original soil shearing resistance.

In the light of this fact, and taking into account the importance of the creep movement at Rwaza, the hypothesis has been formulated that the soil at Rwaza Hill, just as in the experiments mentioned, undergoes some type of soil fatigue leading to a temporary drop in soil resistance.

Therefore a creep experiment has been performed on a reworked sample from the red 'intact' subsoil at Rwaza. One characteristic of a reworked sample is that original bonds between particles are at least partly destroyed. Therefore the measured shearing resistance on such a sample approximates the residual shear strength of the soil material in question. The procedure of the creep experiment was as follows: in the shear box of a mono-axial shearing apparatus, the reworked sample has been exposed to a normal stress of 200 kN m^{-2} and after consolidation a deviator stress of about 70 kN m^{-2} has been added. This deviator stress amounted to about 55 per cent of the one at which the sample currently failed under the mentioned normal stress (Figure 11). After 21 days the upper part of the shearbox has moved 920 microns with respect to the base. Subsequently, the deviator stress has been increased. Rupture occurred at 107 kN m^{-2} instead of the normally expected 136 kN m^{-2}, indicating a drop in residual soil shear strength by about 22 per cent!

This result, however, raises more questions than it solves. Indeed, although there was an appreciable spreading of points, field records of shearing resistance in mottled and crumbled fissure belts have failed to demonstrate the existence of a soil resistance, as low as the one recorded after the creep experiment.

Nevertheless the result is considered as very important for a better understanding of the development of discontinuities in a creeping soil mantle.

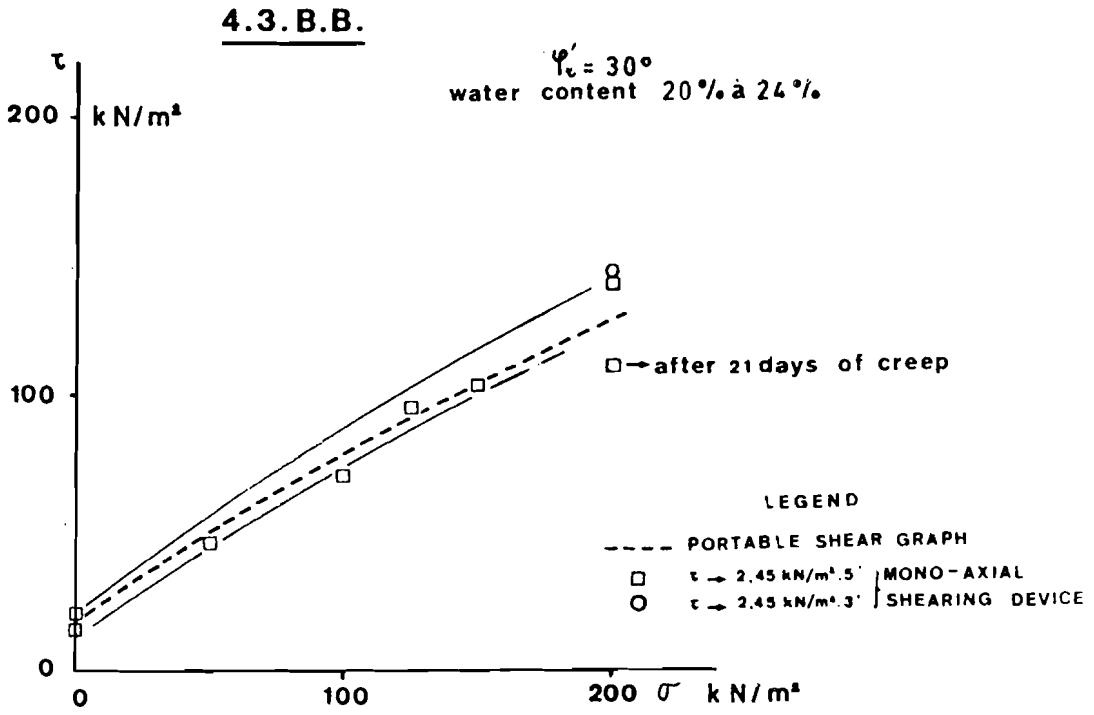

Figure 11. (A) Creep deformation during creep experiment mentioned in text; (B) The residual shear stress of sample 4.3.B.B. after 21 days of creep, compared to the values obtained in tests were creep was restricted in time. In this 'classical' test the deviator stress was increased at a rate of 2·45 kN m^{-2} in 5 or 3 minutes. The tests in the mono-axial shearing apparatus are also compared with a 'quick' test by means of the portable sheargraph

The pattern of potential discontinuities in a creeping soil mantle

Rupture is generally preceeded by creep (Terzaghi, 1950). This movement is composed of an elastic and an inelastic component, the latter being generally considered as plastic (Embleton and Thornes, 1979; Chowdhury, 1978), especially at the prerupture stage where small increments of stress result in important strain. In the case of plane strain, considered here, the plastic flow before rupture is supposed to be parallel to the x–y plane (Figure 12). Once the soil mantle is strained beyond the elastic limit, plastic deformation must fulfil the yield condition (Scheidegger, 1958):

$$\frac{1}{4}(\sigma_x-\sigma_y)^2+\tau_{xy}=k^2 \tag{2}$$

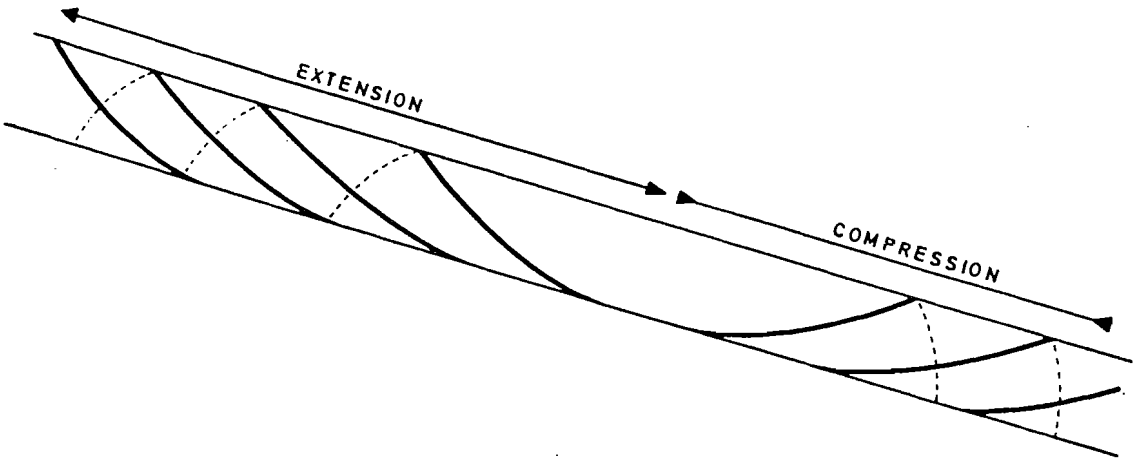

Figure 12. The theoretical configuration of a slip line field in respectively a laterally extending and a laterally compressed belt, according to theory

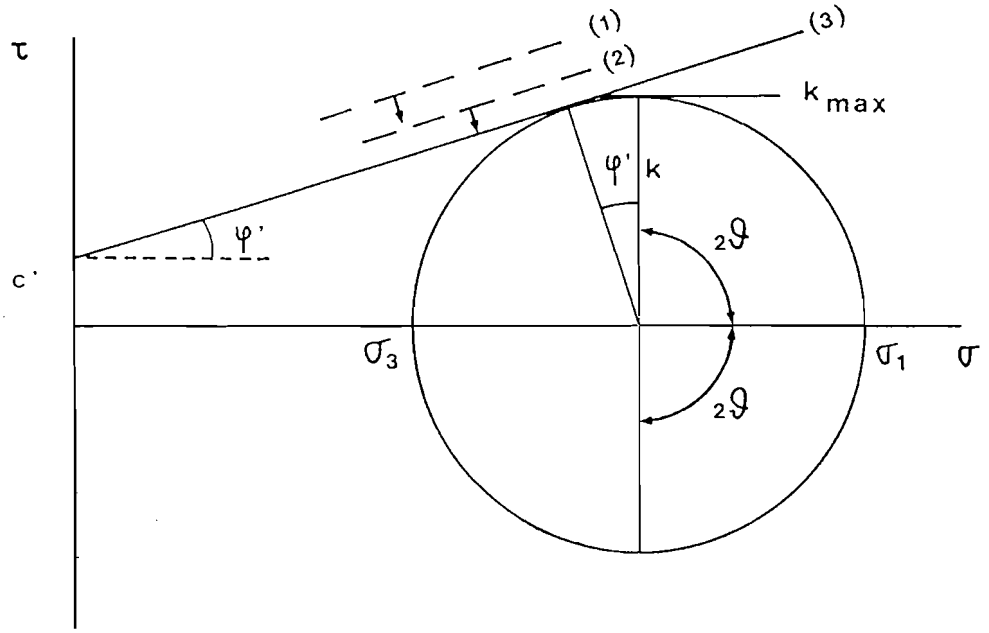

Figure 13. Mohr-circle representing stress state where $\tau_{max}=k$. During the plastic deformation the failure envelope lowers (1), (2), and finally will become tangent to the Mohr-circle (3). During (1) and (2) (plastic deformation) slip lines form an angle of $\vartheta=45°$ with σ_1 direction. At stage (3) the normal to the failure surfaces cross σ_1 at $\vartheta+\varphi/2$.

Here, the symbol k stands for the shear stress at which plastic deformation starts (Figure 13). However, during this deformation, the failure envelope of the soil material, considered as a plastic-rigid substance, lowers and finally becomes tangent to the Mohr-circle with radius k from Equation 2. This situation is also depicted on Figure 13.

Slip-line configurations during prefailure plastic behaviour. Let us now consider the stress state of the soil mantle just before rigid failure, when creep is important (Figure 10B). In theoretical discussions, creep is often represented as a type of laminar movement, or laminar shear, whereby the velocity vectors, eventually decreasing in magnitude with their depth in the soil profile, remain parallel to each other and to the topographical surface (Iveronova, 1964; Kirkby, 1967). But recent investigations at Rwaza (Moeyersons, 1988), amply confirm findings by Finlayson (1981) and Young (1978) that creep movements are much more complex. One of the conclusions from the observations at Rwaza is that volumetric displacements in downslope directions not only differ in time at the same place, but also in place during different periods of measurement. This indicates that portions of a creeping soil mantle will locally undergo lateral compression while at the same time, but in other places, the mantle will extend laterally.

Considering this creep movement as essentially plastic in nature, the analysis of the stress state is analogous to the one, applied by Nye (1951) for the case of plastic glacier flow. Theory provides the possibility of representing the stress field in a plastically creeping mantle by means of slip lines. They are curved lines, following the direction of maximum shear stress (Jaeger and Cook, 1979; Merle, 1984). In a bidimensional stress field as the one of Figure 12, they cross the direction of major stress at $\vartheta=45°$ (Figure 13) which gives rise to two sets of slip lines. These are represented on Figure 12 by the full and dashed lines for belts in lateral extension or compression.

On the base of the above mentioned experiment and data, showing that creep causes a drop in soil shear strength, the slip lines, being orientations of the highest deformation, can be considered as orientations along which the soil will weaken most rapidly and along which rupture will originate and develop first.

It happens that the configuration of lenses of crumbled earth in the terracette landscape of Rwaza 3B is very similar to the pattern of potential failure in a creeping mantle as indicated on Figure 12 by the full line. On Figure 14, structures as seen in a 35 m long trench are represented. Their configuration, compared with the

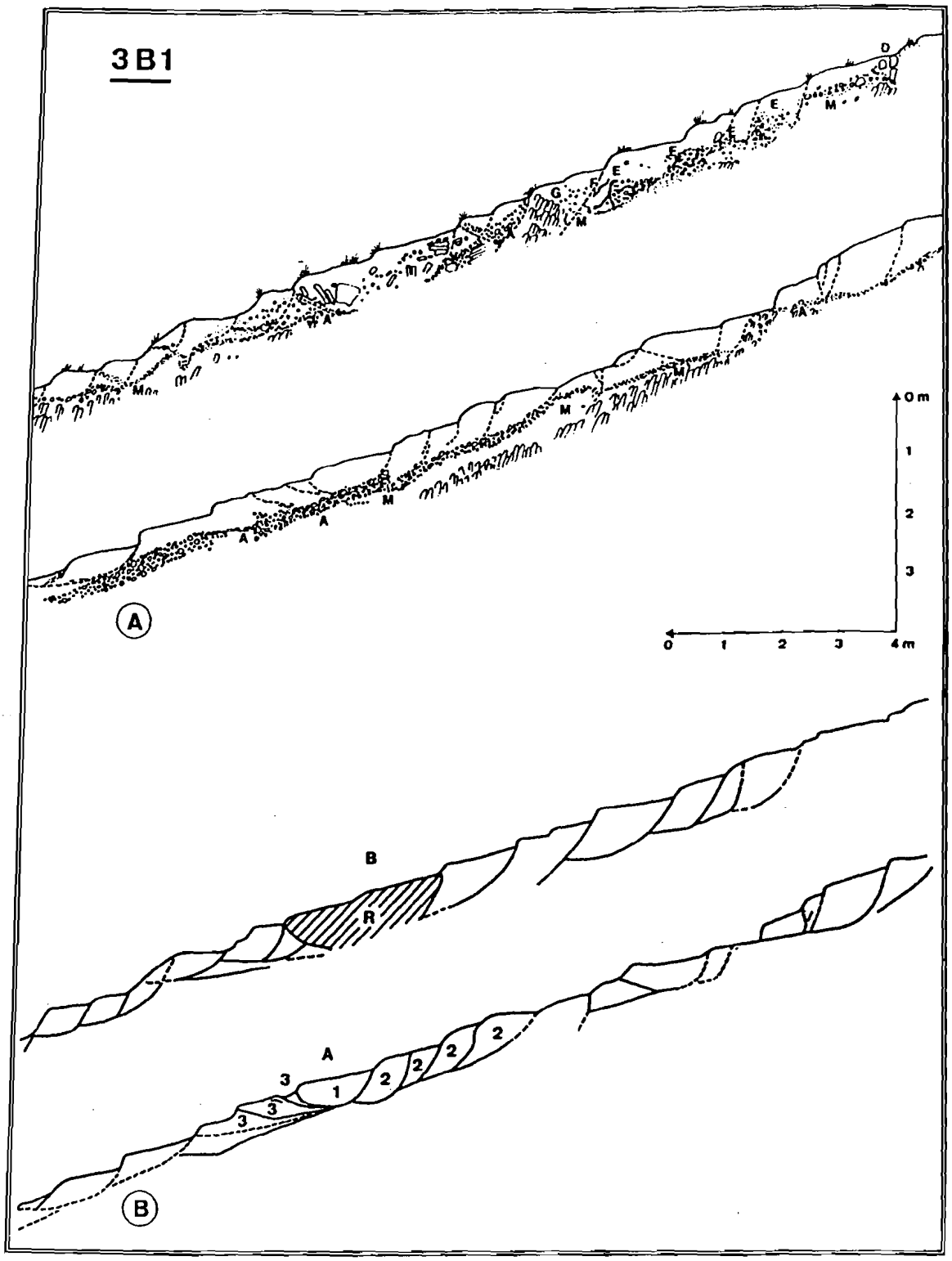

Figure 14. Trench 3B1, on Rwaza 3B. A. Detailed survey of the 35 m long wall; B. The configuration of lenses of crumbled earth, interpreted as slide planes

one on Figure 12 allows to distinguish extension zones: blocks 2 and rotated blocks up the slope of *R*. A compression zone where overthrusting takes or took place comprises blocks 3 and also an area downslope of *R*. However, the latter has been laterally extended later. The configuration of the structures on Figure 7 points essentially to lateral extension.

This close resemblance between theory and the field is an argument pointing to the fact that the actual sliding surfaces follow the orientation of the slip lines, developed during the creep phase where plastic behaviour prevails. However, attention should be paid to the fact that the potential planes of rupture on Figure 12 have to make an angle of 45° with the surface. This follows from the fact that on the surface of a plastically behaving mantle like that on Figure 12 the σ_x- and σ_y- values are equal to σ_1 and σ_3- values of principal stress. Hence, it is known that maximum shear stress is exerted along surfaces making an angle of $\pm 45°$ with the axis of principal stresses $\sigma_1-\sigma_3$ (Jaeger and Cook, 1979). In the field, the pattern of fissures and lenses of crumbled earth shows strong aberrations at this point. In supposed areas of lateral extension, the angle is generally higher than 45°, sometimes it even exceeds 90°. In supposed compression belts, the angle is generally lower than 45°. This difference in theory can be explained by the fact that creep is still continuing on the slopes considered. Hereby, a discontinuity, once formed, will change as indicated on Figure 15 because creep is often more pronounced close to the topographical surface.

The configuration of failure surfaces. Because soil resistance to failure decreases during the creep phase where plastic behaviour prevails, the soil finally will come to the verge of failure. But while slip lines during the plastic behaviour cross the direction of major stress at 45°, the real failure surfaces have to make an angle of $45° - \varphi'_r/2$ (Figure 13) with the same direction (Lambe and Whitman, 1979).

This means that a rupture surface developing along a slip line direction in fact should be composed of a series of microfissures, crossing the slip line direction at an angle of $\varphi'_r/2$ (Figure 16). It becomes clear that the slightest disruption along the slip line direction will cause microdistortion and crumbling. This might explain why terracettes in the field are not separated by single joints but by lenses of crumbled earth.

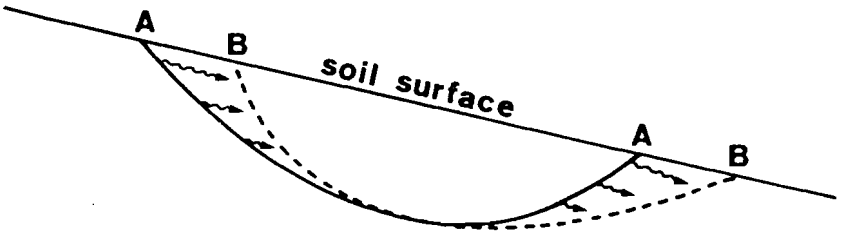

Figure 15. An initial rupture plane (A), showing the orientation of a slip line, and its changed position (B) as a result of creep

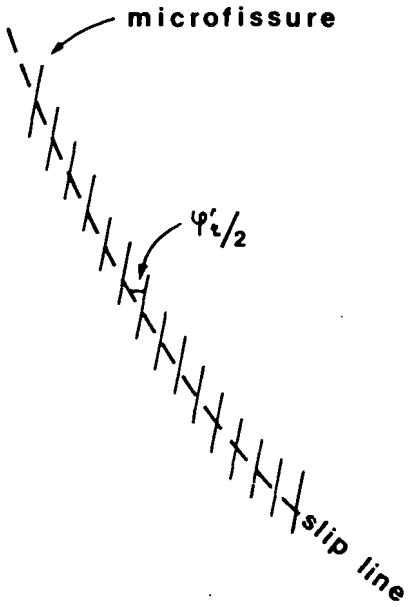

Figure 16. Microfissures developing along a slip line

FINAL DISCUSSION

From the foregoing, it appears that two arguments support the hypothesis that creep can trigger slow sliding, leading to terracette formation, even if the acting shear stresses are below the residual shear strength recorded in the lenses of crumbled earth.

1. The creep experiment reported, indicates that creep can reduce the soil resistance till below the residual one. In this way seepage is not needed to induce motion.
2. The pattern of the slide surfaces in the field shows very close affinities with the pattern of slip lines predicted by theory in a creeping mantle where plastic behaviour prevails.

The question arises of how the soil resistance, after its theoretical lowering till below the residual one by creep, can increase again to the level of the residual shear strength as measured in the field in the lenses of crumbled earth.

In order to find an answer to this question, let us follow, in chronological order, the events occurring on a creeping slope (Figure 17).

A. Let us start from a situation where the soil material possesses its original shear strength (A on Figure 17). If this material rests on a slope, a shear stress, R, eventually higher than the fundamental shear strength (Griggs, 1936) but lower than the Mohr shear strength will be imposed by gravity, and creep starts. On Figure 17 it is suggested that the soil resistance lowers during creep deformation. This drop in resistance, mentioned by Zaruba and Mencl (1976), is probably caused by the gradual reorientation of the clay pellets in the soil. Authors such as Goldstein *et al.* (1961) and Skempton (1964) found, indeed, that in creeping soil material clay pellets start to be reoriented following the direction of highest deformation long before rupture occurs. From the definition of slip lines it can be assumed that the orientation of the clay pellets should reflect the directions of slip lines. The drop of soil resistance, indicated on Figure 17 should be an anisotropic phenomenon, following the slip line orientations.

B. If time is long enough, the soil shear strength along slip line directions will become as low as the acting shear stress. This happens in point 0 at the t_0. From this moment on, progressive rupture (Bjerrum, 1967) following the slip line orientations can occur.

C. However, as the initial rupture in fact has to be composed of a high number of in echelon fissures (Figure 16), displacements necessarily lead to the development of a crumbled belt instead of a single plane fissure. It seems logical that the movement in the first instance only has to overcome a shearing resistance close to the one which can be mobilized along each of the microfissures indicated on Figure 16. But a continuation of the movement very soon leads to distortion and crumbling, as explained higher, which

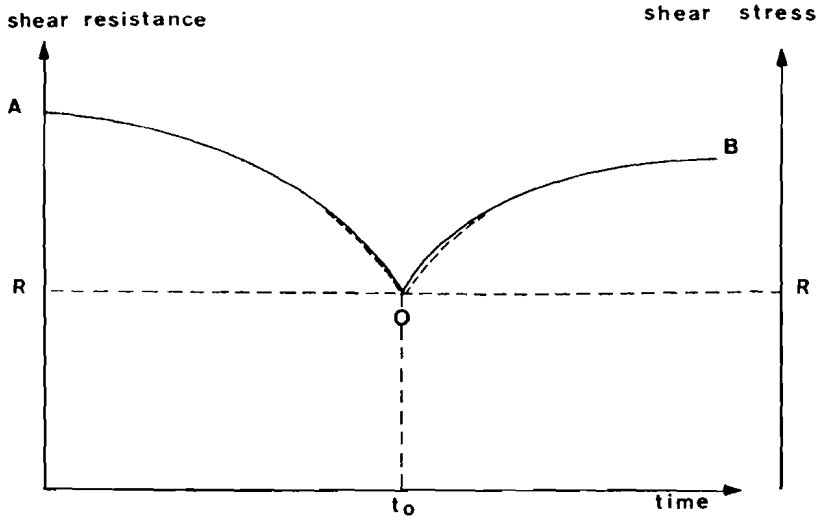

Figure 17. The inferred evolution of the shearing resistance along a plane of weakness in development

creates a sliding plane of more irregular microform. This certainly is a factor contributing to an increasing shear resistance. It depends from the level of the acting shear stress at what displacement distance the shear stress will be balanced by the increasing shear strength. Taken the dimensions of the microfissures, possibly of the centimetre order, displacements of the same order of magnitude should generate the development of a lense of crumbled earth. It is interesting to see that creep in this stage will contribute to further instability because of the continuing deformation of the original composite rupture plane from Figure 16 as illustrated on Figure 15. Hereby the inclination of the initial rupture line becomes steeper in extension zones while the counterslope decreases in compression zones. Because of the slowness of the creep movement, increase of shear stress by this deformation is slow. This explains a slow adjustment, translated by the slow movements between terracettes as recorded in the field.

CONCLUSION

The coexistence of creep and sliding on slopes on the verge of failure is not a new element. Terzaghi mentioned already in 1950 that creep generally preceeds and follows sliding. In this article, it is argued that creep prepares the soil to sliding by:

1. Temporarily diminishing the soil resistance
2. By determining the embryonic pattern of the potential sliding planes.

In this respect, creep can be considered as the ultimate cause of sliding. Only in cases where shear stresses occur higher than the residual soil shear strength sudden failures, poorly announced by creep, have to be feared. In natural situations, the general shear stress level should be lower than the general residual soil shear strength because slope form has had enough geological time to reach an equilibrium with the existing stress field. Therefore a reactivation of sliding, as it seems to happen on the steep sloping grounds in Rwanda, seems to point to an activation, eventually caused by human intervention, of soil creep. If this is true, the findings in this article open the door for a new approach of preventive treatment of slopes against sliding by looking to methods able to freeze creep movements.

ACKNOWLEDGEMENTS

This research was possible in the context of a convention between Belgium and Rwanda of the Royal Museum of Central Africa (Tervuren-Belgium) and the 'Institut National de Recherche Scientifique' (Butare-Rwanda). I wish to express my gratitude to both institutions. I am also grateful to Prof. J. De Ploey who allowed me to perform creep and shearing tests in the Laboratory of Experimental Geomorphology of the K.U. Leuven.

REFERENCES

Anderson, M. G., Kemp, M. J. and Shen, J. M. 1987. 'On the use of resistance envelopes to identify the controls on slope stability in the tropics', *Earth Surface Processes and Landforms*, **12**, 637–648.

Bishop, A. W. 1955. 'The use of the slip circle in the stability analysis of slopes', Géotechnique, **5**, 7–17.

Bjerrum, L. 1967. 'Progressive failure in slopes of overconsolidated plastic clay and clay shales', J. Soil Mech. and Found. Division A. S. C. E., **93**, SM 5, Proc. Paper 5456, 149 pp.

Chowdhury, R. N. 1978. 'Slope analysis', *Developments in Geotechnical Engineering*, **22**, Amsterdam, 423 pp.

Embleton, C. and Thornes, S. 1979. *Process in Geomorphology*, London, 436 pp.

Fellenius, W. 1936. *Calculation of Stability of Earth Dams*, Transactions 2nd Congress Large Dams, 4, 445 pp.

Finlayson, B. 1981. 'Field measurements of soil creep', *Earth Surface Processes and Landforms*, **6**, 35–48.

Goldstein, M. N., Misumsky, V. A., and Lapidus, L. D. 1961. 'The theory of probability and statistics in relation to the rheology of soils', *Proc 5th Int. Conf. on soil Mech. Found. Engng.*, 123–126.

Griggs, D. T. 1936. 'Deformation of rocks under high confining pressures', *Journal of Geology*, **44**, 541–577.

Iveronova, M. I. 1964. 'Stationary studies of the recent denudation processes on the slopes of the R. Tchon–Kizilsu basin, Tersky Alatan Ridgem Tien-Shan', *Z. f. Geomorphologie, S. B.* **5**, 206–212.

Jaeger, J. C. and Cook, N. G. W. 1979. *Fundamentals of Rock Mechanics*, London, 593 pp.

Kirkby, M. J. 1967. 'Measurement and theory of soil creep', *Journal of Geology*, **74**, 4, 359–378.

Lambe, T. W. and Whitman, R. V. 1979. *Soil Mechanics*, S. I. Version, New York, 553 pp.

Merle, O. 1984. 'Déplacement et déformation des nappes superficielles', *Revue de Géologie Dynamique et de Géographie Physique*, **25**, 1, 3–17.
Moeyersons, J. 1988: 'The complex nature of creep movements on steeply sloping ground in Southern Rwanda', *Earth Surface Processes and Landforms*, **13**, in press.
Nye, J. F. 1951. 'The flow of glaciers and ice sheets as a problem in plasticity', *Proc. Roy. Soc. Lond.*, **a.207**, 554–572.
Scheidegge, I. E. 1958. *Principles of Geodynamics*, Berlin, 280 pp.
Skempton, A. W. 1964. 'Long-term stability of clay slopes', *Geotechnique*, **14**, 77–102.
Skempton, A. W. and Delory, F. A. 1957. 'Stability of natural slopes in London Clay', *Proc. 4th Int. Conf. Soil Mech., London*, **2**, 378–381.
Terzaghi, K. 1950. 'Mechanism of landslides', *Geol. Soc. Am. Eng. Geology*, Vol. 83–123.
Young, A. 1960. 'Soil movement by denudational processes on slopes', *Nature*, **188**, 120–122.
Young, A. 1978. 'A twelve-year record of soil movement on a slope', *Z. f. Geomorphologie, S. B.* **29**, 104–110.
Zaruba, G. and Mencl, V. 1976. *Engineering Geology*, Elsevier Amsterdam, 504 pp.